

**NATURAL RADIATION HAZARDS ON THE MANNED MARS MISSION**

John R. Letaw, Rein Silberberg, C.H. Tsao

E.O. Hulbert Center for Space Science  
Naval Research Laboratory  
Washington, DC**ABSTRACT**

We consider the hazards of the natural radiation environment--cosmic rays and solar energetic particles--on a manned mission to Mars. These hazards are addressed in three different settings: (1) the flight to Mars where astronauts are shielded only by the spacecraft, (2) on the surface of Mars under an atmosphere of about  $10 \text{ g/cm}^2$  carbon dioxide, and (3) under the surface of Mars where additional shielding would result.

**INTRODUCTION**

The manned mission to Mars is confronted with a high energy nuclear radiation exposure two orders of magnitude greater than that encountered on previous space missions. The dose rate is comparable to what Apollo astronauts received on Moon missions; however, the flight duration is expected to be about 3 years, or 100 times longer than the average 10 day Moon mission. Longer space flights, such as Skylab, are not comparable to the Mars mission because they were not exposed to the full force of the radiation environment.

A baseline dose equivalent rate for the Mars spaceflight is 43 rem/year. This is based on a computation (Silberberg et al., 1984) of the free space cosmic ray flux just under the surface (0.1 cm) of a 30 cm diameter sphere of water. The natural radiation environment of Adams et al. (1981) was used as a model of the cosmic ray flux ( $Z < 29$ ) at solar minimum. The model does not accurately predict free space cosmic ray fluxes at energies  $< 10 \text{ MeV/nucleon}$ , but these particles are removed by very thin shielding. Particles surviving 0.1 cm of water originate at energies above this limit.

The baseline dose as described here maintains a fairly continuous intensity. The solar cycle introduces downside variations of about a factor of 2 in integral fluxes above 150 MeV/nucleon, and up to a factor of 10 in low energy fluxes. Aluminum shielding ( $4\text{g/cm}^2$ ) reduces the dose to about 36 rem/year. Self-shielding of the spherical phantom reduces the dose to about 24 rem/year at its center. The baseline dose is

essentially inevitable. Energetic particles associated with solar flares are the primary risk of higher dose rates. This risk is not presently quantified and is strongly dependent on shielding.

The expected dose equivalent rate on the surface of Mars is reduced from the baseline a factor of 2 by shielding with the planet's mass. Further attenuation results from atmospheric shielding. For an assumed vertical atmospheric depth of  $10 \text{ g/cm}^2$  the dose equivalent rate due to cosmic ray primaries is estimated to be 10 rem/year. Neutrons should not be an appreciable fraction of the dose at this depth - we guess neutrons would increase the surface dose by no more than 25%. We suggest the surface dose equivalent is 12 rem/year.

Under Martian soil, the dose continues to fall, perhaps by a factor of 2 from the surface to  $20 \text{ g/cm}^2$  ( $\sim 10 \text{ cm}$ ) below the surface. Another reduction by a factor of 2 can be expected down to  $60 \text{ g/cm}^2$  ( $\sim 30 \text{ cm}$ ) below the surface. At this depth, neutrons dominate the dose equivalent and further reductions are not so rapid. We have not estimated the neutron dose under the surface.

#### CONCEPTS: THE NATURAL RADIATION ENVIRONMENT

The natural radiation environment encountered on a mission to Mars consists primarily of galactic cosmic rays and solar energetic particles.

Galactic Cosmic Rays: (a) Mostly protons, 10% He, 1% heavier ions; (b) Hard spectrum ( $E^{-2.2}$  for protons); (c) Relatively constant intensity (factor of 2-3 variation with solar cycle); and (d) High energy (mean about 2 GeV/nucleon).

Solar Energetic Particles: (a) Mostly protons, variable heavy ion composition usually not as rich as cosmic rays; (b) Soft spectrum ( $E^{-5}$  or so for protons); (c) Widely varying intensity (many orders of magnitude); (d) Low energy (mean  $< 100 \text{ MeV/nucleon}$ ); and (e) Unpredictable.

Figure 1 shows the differential proton energy spectrum for cosmic rays at solar minimum and solar maximum, and for a large solar event (4-7 Aug 1972). The cosmic ray spectra are integrated over a week, while the solar protons are integrated over the flare duration. Above a few GeV/nucleon there is no solar cycle variation. Low energy fluxes vary by up to a factor of 10. Integral fluxes above 100 MeV/ nucleon vary by factors of 2 or 3.

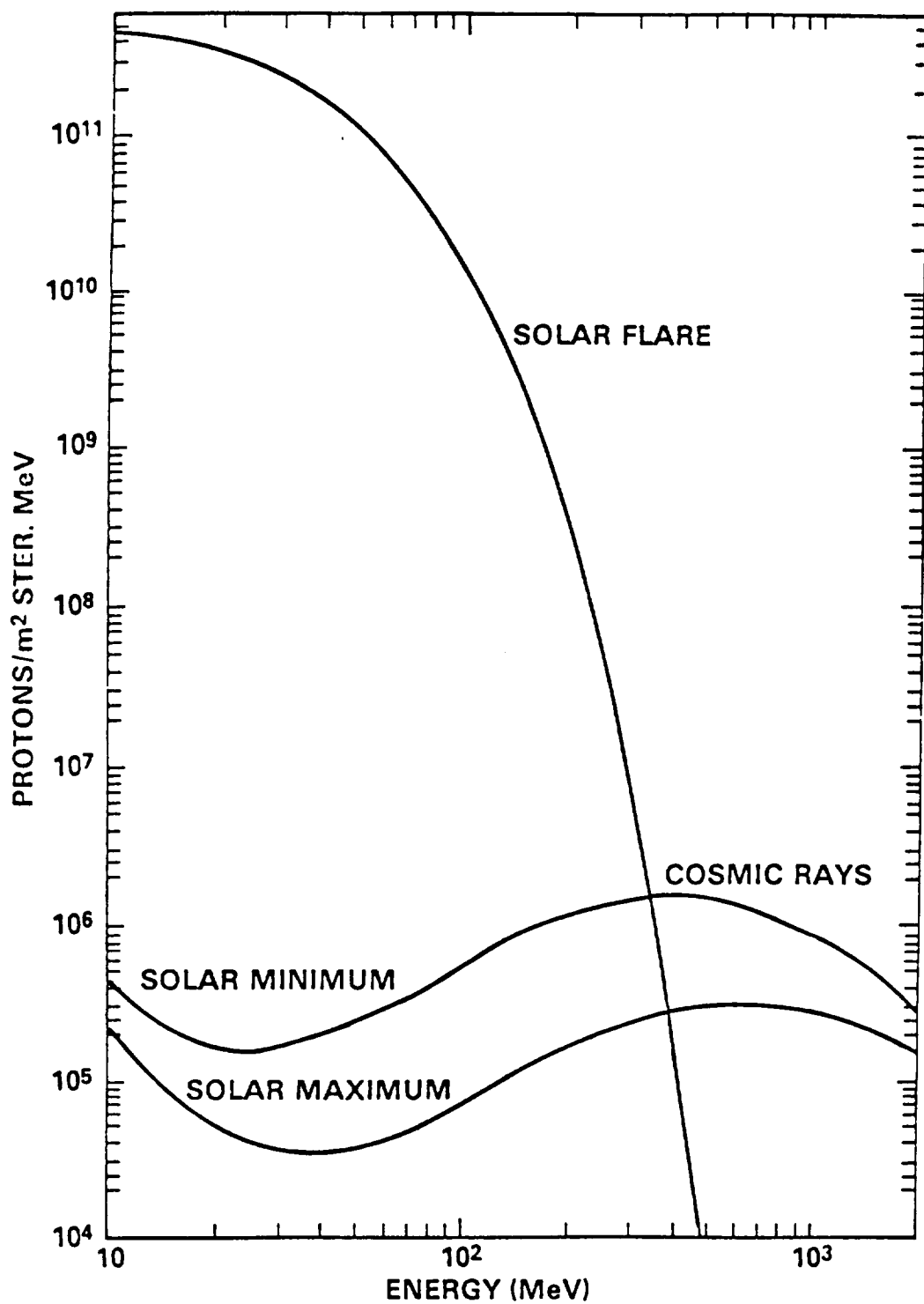


FIGURE 1

How well do we understand the environment? We can predict the galactic cosmic ray fluxes to within a factor of 2, well ahead of time. After the fact, much better estimates of the accumulated dose should be possible by examination of data from satellite-borne particle monitors. There is no complete engineering model of the risks associated with solar energetic particles. Important factors in such a model would be peak intensity, duration, energy spectrum, heavy ion enrichment, and time-intensity profile. All of these factors are critical for estimates of the biological risks of solar energetic particles.

It is worth noting that we are interested in the natural particle environment in the vicinity of Mars. This differs in several ways from the environment around Earth. The cosmic ray flux at 1.5 AU is somewhat greater than at Earth. Measurements from Pioneer 10 and 11 (McKibben et al. 1983) show radial gradients of 3-4%/AU at solar minimum at energies > 67 MeV. Below this energy, variations of up to 15%/AU have been observed. Mars also has a negligible magnetic field. The associated magnetic rigidity cutoff, which protects astronauts in low inclination orbits around Earth from most cosmic rays, is missing. In addition, there is no trapped radiation presenting a risk of high dose in Mars orbit.

#### CONCEPTS: PARTICLE TRANSPORT AND SHIELDING

Astronauts are never exposed to free space radiation intensities. In addition to the shielding provided by space vehicles and suits, self-shielding provides some protection. An example of self-shielding is shown in Figure 2. This is the pathlength distribution 0.1 cm below the surface of a 30 cm spherical phantom as used in computing the baseline dose in free space. Figure 2 shows an exposure of 3.16 steradians through less than 0.2 cm shielding. On the other hand, cosmic rays are shielded by between 6.0 and 30 cm of water (uniformly distributed) over 40% of the solid angle.

We would like to understand the properties of shielding to guide us in defining structures and procedures for protecting astronauts from space radiation. To understand the effects of shielding, we must understand the transport of high energy nuclei in materials. Much work has been done in this field (see, for example, Letaw et al. 1984, Letaw et al. 1983, Silberberg and Tsao 1973). We briefly explore several concepts below.

3631-86

## SPHERICAL PHANTOM PATHLENGTH DISTRIBUTION

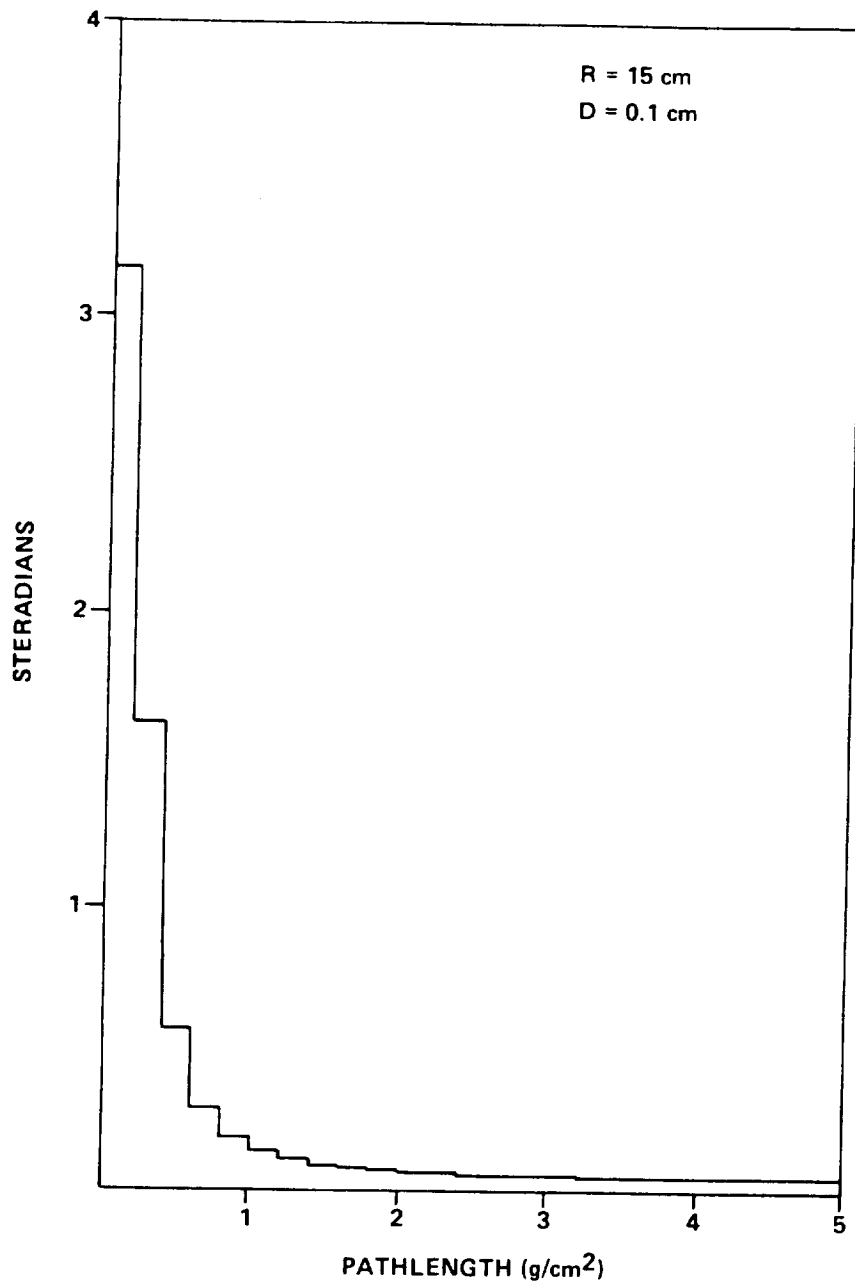


FIGURE 2

There are two important mechanisms for degrading high energy particle fluxes in matter: (1) ionization loss, and (2) nuclear fragmentation. Ionization loss is a continuous slowing down of charged particles introduced by their collisions with atoms. It effectively gives the charged particles a finite and well-defined range in materials. Table 1 shows the ranges of several ions at several energies in water, aluminum, and carbon dioxide. The table shows that: (a) Shielding materials consisting of lighter atoms are more effective at stopping fast ions, and (b) A few g/cm<sup>2</sup> of shielding has essentially no effect on most cosmic rays (> 1 GeV/N), but stops the heavy ions (and much of the proton flux) from solar energetic particle events.

Table 2 shows approximate interaction mean free paths for several ions in several materials. Unlike ionization loss rates, the interaction mean free paths are roughly independent of energy. Table 2 shows that: (a) Shielding materials consisting of lighter atoms are effective at degrading heavy ions by fragmentation, and (b) At some energy below 1 GeV/nucleon, nuclear fragmentation is a more efficient degradation mechanism than ionization loss.

One additional factor not comprehended in the Tables is the buildup of neutrons. Especially in materials of high molecular weight, neutrons are released from the target nuclei in ion interactions. The majority of the neutrons are released in proton nucleus interactions. Neutron buildup is best treated with an intranuclear cascade code (for example, Armstrong and Chandler, 1972).

#### CONCEPTS: DOSE ESTIMATION

Particle transport codes give high energy particle fluxes at any point within a structure or a body. The biological effects of this radiation are estimated by computing the rate of energy deposition by each particle type at each energy. A quality factor compensates for the increased damage associated with higher density of energy deposition. We use the following integral to compute dose equivalent:

$$D(S) = \int J(S) Q(S) S dS$$

where  $J(S)$  is the flux of particles having LET of  $S$  and  $Q(S)$  is the quality factor associated with LET of  $S$ .

$$\begin{aligned} Q(S) = & 1 & S < 35 \text{ MeV}/(\text{g/cm}^2) \\ & 0.072S - 0.74 & 35 < S < 2000 \\ & 20 & S > 2000 \end{aligned}$$

TABLE 1  
RANGES OF IONS IN MATERIALS (G/CM<sup>2</sup>)

		H <sub>2</sub> O	CO <sub>2</sub>	Al
H :	30 MeV/N	0.9	1.0	1.2
	100 MeV/N	7.7	8.9	10.0
	1 GeV/N	330.0	370.0	410.0
	10 GeV/N	4700.0	5100.0	5800.0
C :	30 MeV/N	0.3	0.35	0.4
	100 MeV/N	2.6	3.0	3.3
	1 GeV/N	110.0	120.0	140.0
	10 GeV/N	1600.0	1700.0	1900.0
Mg :	30 MeV/N	0.16	0.18	0.21
	100 MeV/N	1.3	1.5	1.7
	1 GeV/N	54.0	61.0	68.0
	10 GeV/N	780.0	840.0	950.0
Fe :	30 MeV/N	0.09	0.11	0.12
	100 MeV/N	0.67	0.78	0.90
	1 GeV/N	27.0	30.0	33.0
	10 GeV/N	380.0	410.0	470.0

Note: This table is based on theoretical calculations and empirical fits known to be approximately correct. It has not been checked explicitly against measurements.

TABLE 2  
INTERACTION MEAN FREE PATHS OF IONS IN MATERIALS (G/CM<sup>2</sup>)

	H <sub>2</sub> O	CO <sub>2</sub>	Al
H	74	84	99
He	36	40	51
C	19	25	34
Mg	13	18	25
Fe	8	11	16

All values are given at 1 GeV/nucleon. Variations of up to a factor of 2 occur at lower energies down to 10 MeV/nucleon. Little variation occurs above 1 GeV/N.

Note: This table is based on theoretical calculations and empirical fits known to be approximately correct. It has not been checked explicitly against measurements.

This is our parameterization. Note that relativistic protons have  $S = 2$ , relativistic C has  $S = 72$ , slow protons (a few MeV) have  $S = 100$ , relativistic Fe has  $S = 1400$ , and all cosmic rays of interest have  $S < 105$ .

It is important to note that relativistic Fe is thousands of times more damaging than relativistic protons (using our quality factor). Slow Fe, for example from a heavy ion rich solar flare, is tens of thousands of times more damaging than the minimum ionizing particles. We emphasize the most effective shielding is the (approximately)  $5 \text{ g/cm}^2$  needed to eliminate heavy ions from solar flares and low energy cosmic rays.

#### RESULTS

We have previously (Silberberg et al. 1984) calculated the dose equivalent rate to a 30 cm spherical phantom at various depths. Results are shown in Figures 3 and 4. Figure 3 shows the free space exposure. A rate of 36 rem is taken from the 0.1 cm depth. To this is added an estimated neutron dose of 7 rem to give our baseline of 43 rem. Figure 4 is the same dose calculation except under  $4 \text{ g/cm}^2$  aluminum shielding. This shielding thickness is thought to be typical of spacecraft. The maximum cosmic ray dose in Figure 4 is 26 rem, to which we add 10 rem for neutron buildup in the shielding. Little reduction in dose is associated with shielding.

Figure 5 shows the relative contributions of various charge groups to the dose equivalent. Note that heavy ions are the most important component of the dose at all depths.

During the writing of this report, we have recomputed the baseline dose in free space. This recalculation was suggested by the many improvements in our transport codes and particle environment models over the past few years. We quote a preliminary result of 47 rem for the cosmic ray primary dose, to which must be added 7 rem from neutrons. Thus the baseline dose may be as high as 54 rem. We emphasize the preliminary nature of this result which is given as a guide to the uncertainty of our calculations.

Figure 6 shows the dose equivalent rate (per solid angle) at slab depths of up to  $60 \text{ g/cm}^2$  CO<sub>2</sub>. Cosmic rays at solar minimum in the charge range  $Z < 29$  were used as the incident flux. The "zero" depth point is actually under  $0.1 \text{ g/cm}^2$  so very low energy fluxes have been removed.

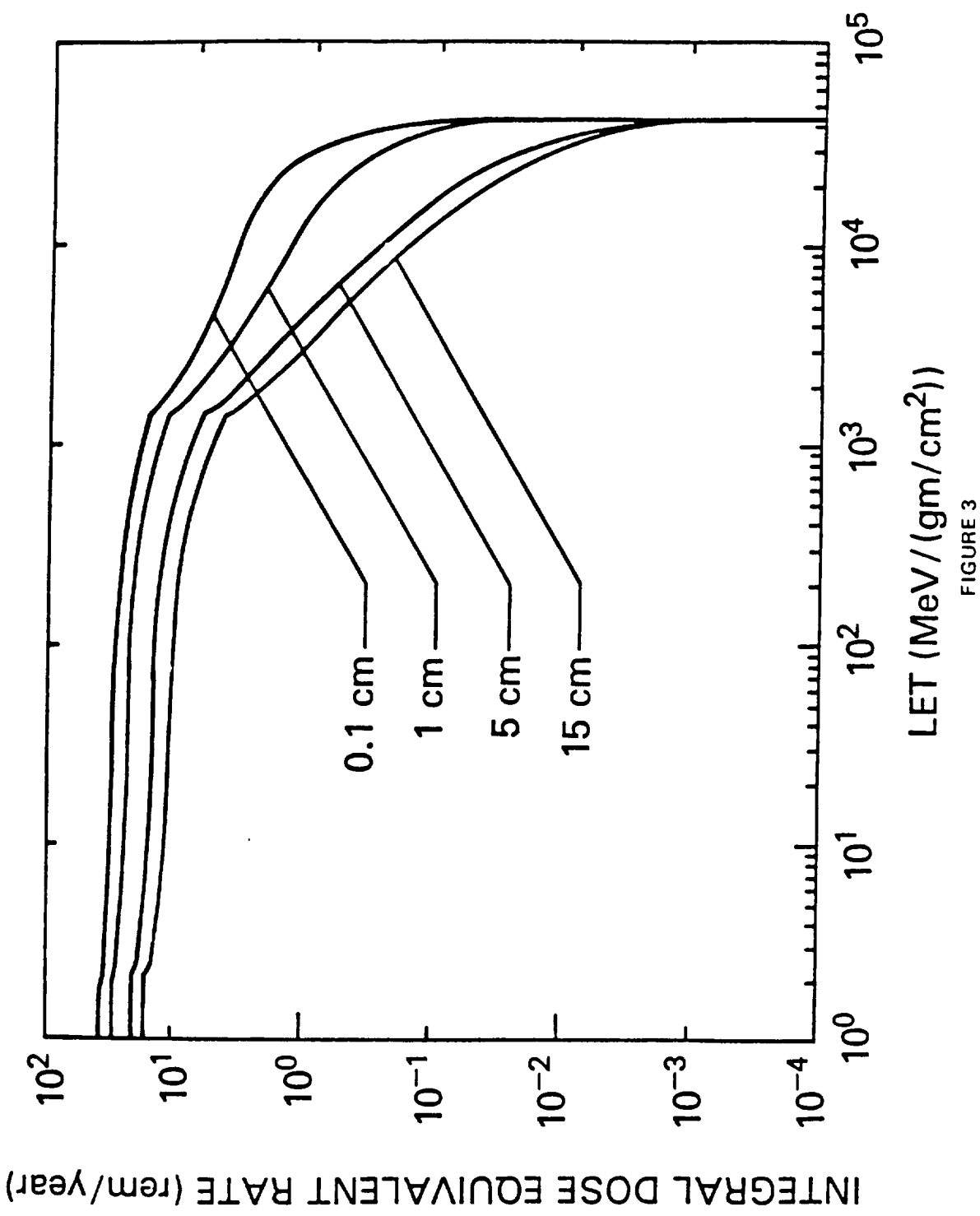
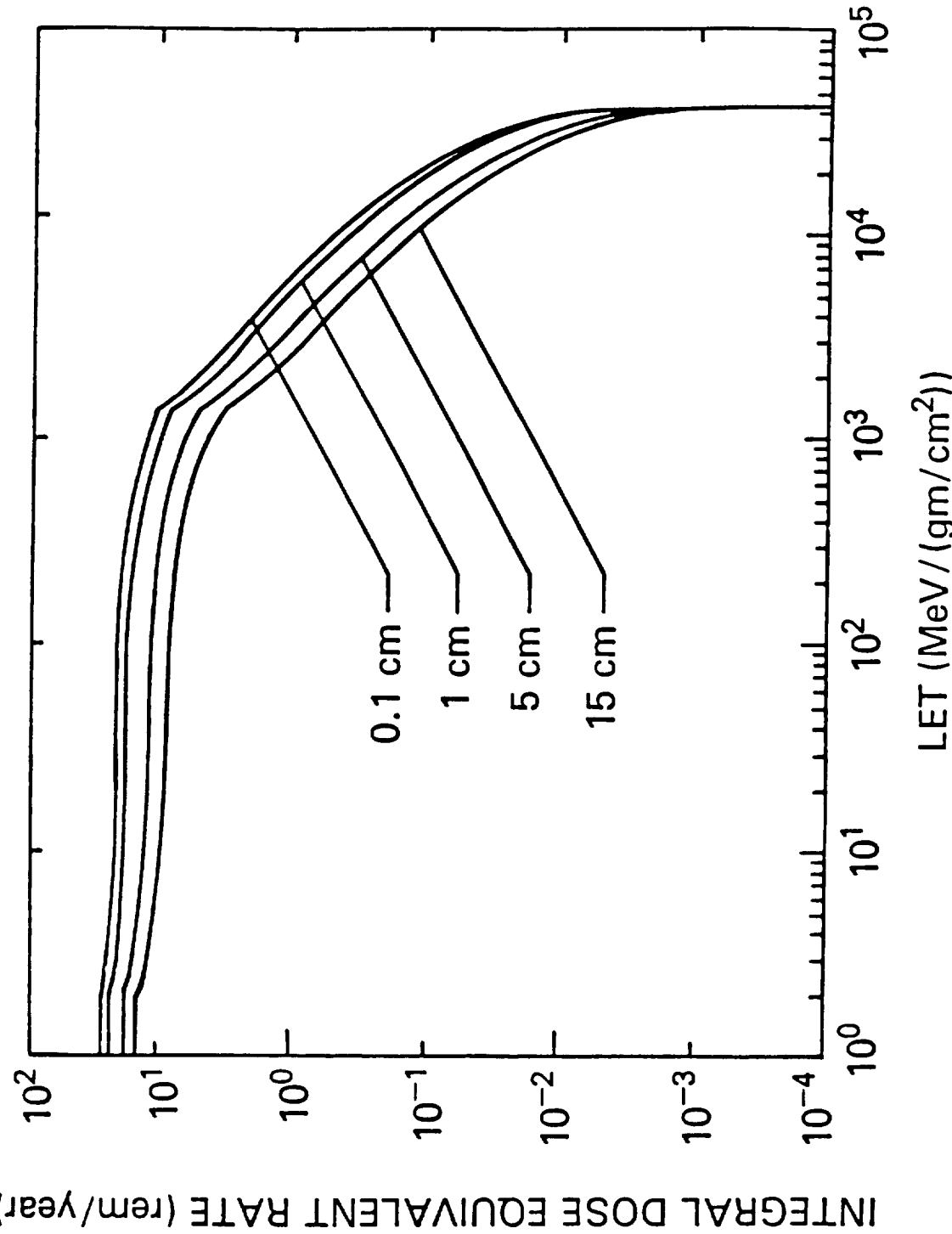


FIGURE 3

FIGURE 4



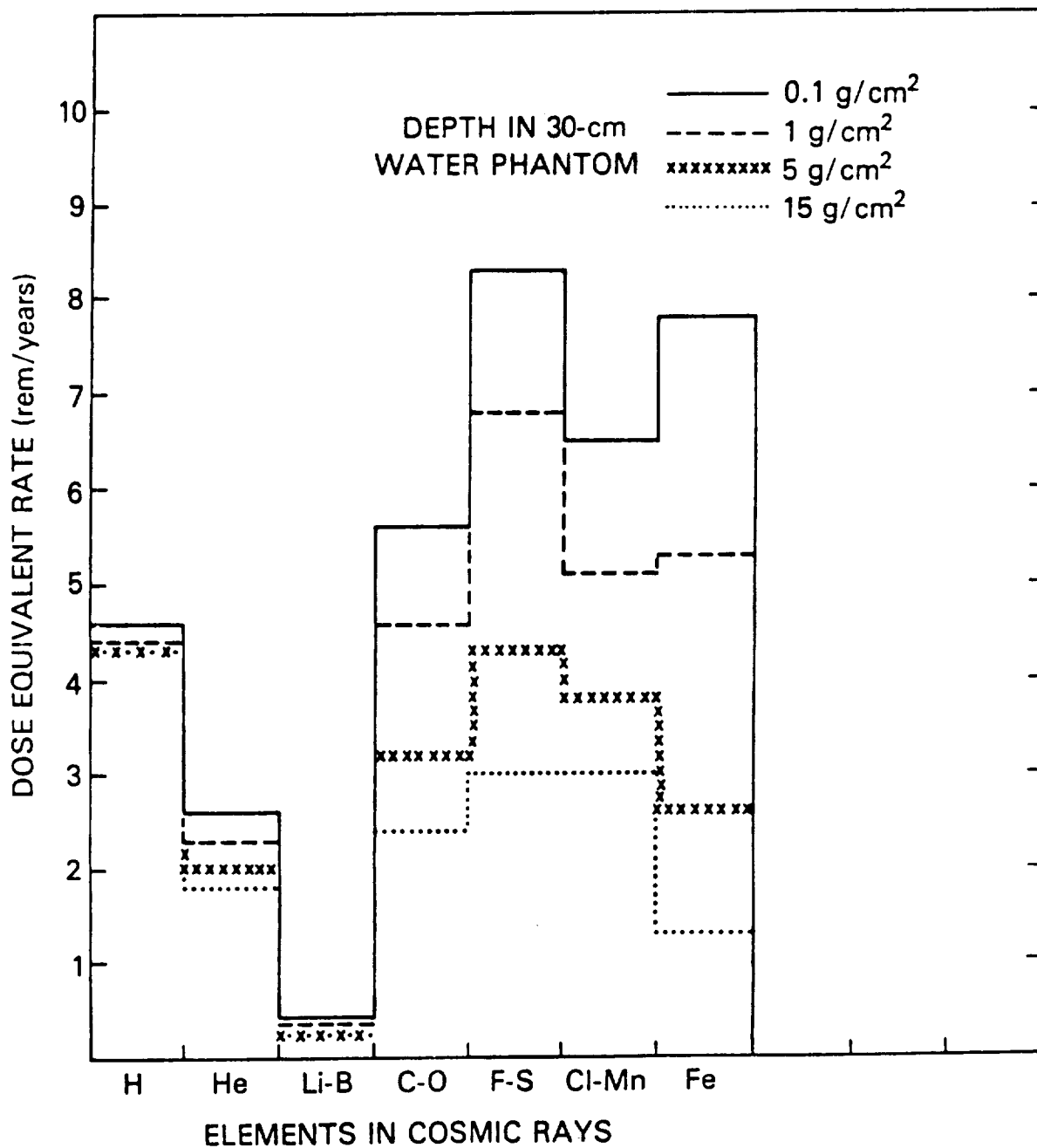


FIGURE 5

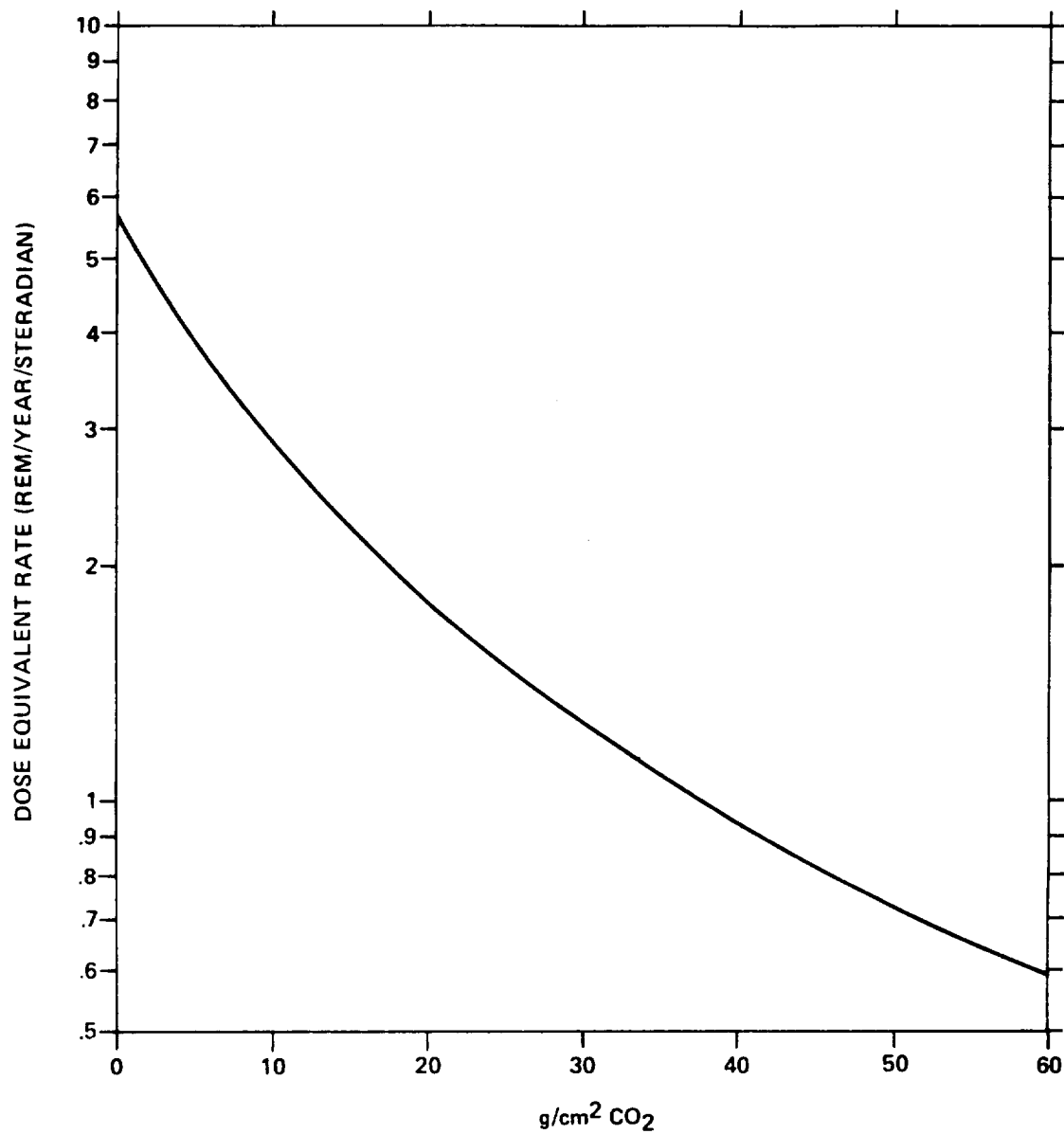


FIGURE 6

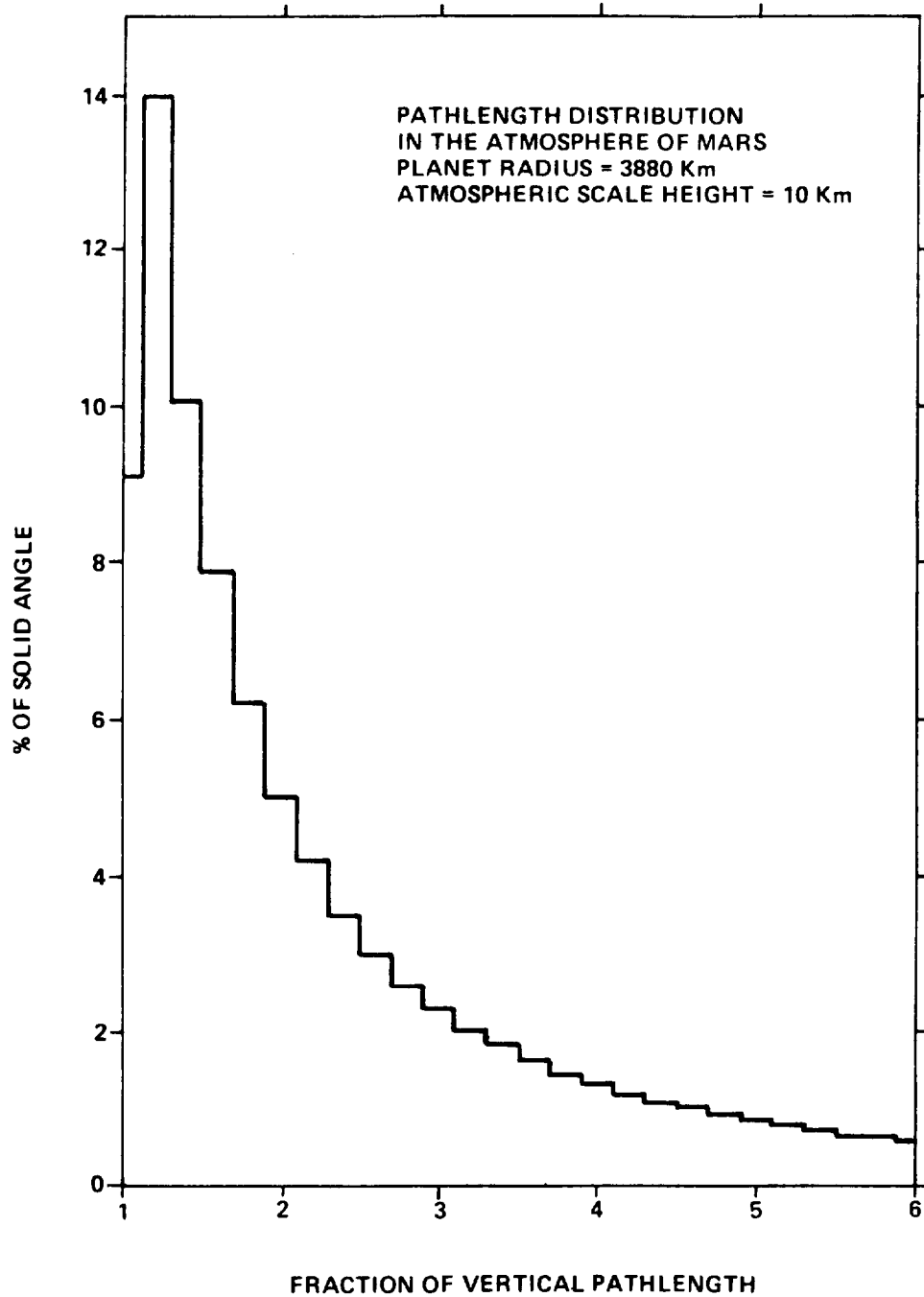


FIGURE 7

Figure 7 shows the pathlength distribution in the martian atmosphere. Since the vertical depth is variable and uncertain, the function is described in terms of fractions of this pathlength. An atmospheric scale height of 10 km was used to determine the distribution, though the results are insensitive to the scale height. Combining Figures 6 and 7 (with an overall factor of 2 pi steradians) gives a total cosmic ray dose at the planet's surface of 10 rem/year. We estimate a contribution of about 2 rem/year giving a surface dose of 12 rem/year.

#### REFERENCES

1. Adams, J.H., Silberberg, R., and Tsao, C.H. 1981, Cosmic Rays Effects on Microelectronics Part I: The Near Earth Particle Environment, NRL Memorandum Report 4506.
2. Armstrong, T.W. and Chandler, K.C. 1972, Nucl. Sci. Eng. 49, 110.
3. Letaw, J.R., Silberberg, R., and Tsao, C.H. 1983, Ap. J. Suppl. 51, 271.
4. Letaw, J.R., Silberberg, R., and Tsao, C.H. 1984, Ap. J. Suppl. 56, 369.
5. McKibben, R.B., Pyle, K.R., and Simpson, J.A. 1983, 18th Int. Cosmic Ray Conf., MG 2.2-6.
6. Silberberg, R., and Tsao, C.H. 1973, Ap. J. Suppl. 25, 315.
7. Silberberg, R., Tsao, C.H., Adams, J.H., and Letaw, J.R. 1984, Rad. Res. 98, 209.